Molecular Therapy
Methods & Clinical Development
Original Article

Systemic gene therapy using an AAV44.9 vector rescues a neonatal lethal mouse model of propionic acidemia

Randy J. Chandler,[1] Giovanni Di Pasquale,[2] Eun-Young Choi,[1] David Chang,[1] Stephanie N. Smith,[1] Jennifer L. Sloan,[1] Victoria Hoffmann,[3] Lina Li,[1] John A. Chiorini,[2] and Charles P. Venditti[1]

[1]National Human Genome Research Institute, Bethesda, MD 20892, USA; [2]National Institute of Dental and Craniofacial Research, Bethesda, MD 20892, USA; [3]Office of Research Services, National Institutes of Health, Bethesda, MD 20892, USA

Propionic acidemia (PA) is rare autosomal recessive metabolic disorder caused by defects in the mitochondrially localized enzyme propionyl-coenzyme A (CoA) carboxylase. Patients with PA can suffer from lethal metabolic decompensation and cardiomyopathy despite current medical management, which has led to the pursuit of gene therapy as a new treatment option for patients. Here we assess the therapeutic efficacy of a recently described adeno-associated virus (AAV) capsid, AAV44.9, to deliver a therapeutic *PCCA* transgene in a new mouse model of propionyl-CoA carboxylase α (PCCA) deficiency generated by genome editing. *Pcca*$^{-/-}$ mice recapitulate the severe neonatal presentation of PA and manifest uniform neonatal lethality, absent PCCA expression, and increased 2-methylcitrate. A single injection of the AAV44.9 PCCA vector in the immediate newborn period, systemically delivered at a dose of 1e11 vector genome (vg)/pup but not 1e10 vg/pup, increased survival, reduced plasma methylcitrate, and resulted in high levels of transgene expression in the liver and heart in treated *Pcca*$^{-/-}$ mice. Our studies not only establish a versatile and accurate new mouse model of PA but further demonstrate that the AAV44.9 vectors may be suitable for treatment of many metabolic disorders where hepato-cardiac transduction following systemic delivery is desired, such as PA, and, by extension, fatty acid oxidation defects and glycogen storage disorders.

INTRODUCTION

Propionic acidemia (PA) is a well-recognized autosomal recessive disorder of organic acid metabolism, occurring with an estimated incidence of 1:250,000–1:750,000 births.[1,2] It is caused by a deficiency of propionyl-coenzyme A (CoA) carboxylase (PCC), a ubiquitously expressed, mitochondrial enzyme involved primarily in the catabolism of propiogenic amino acids, particularly isoleucine, valine, methionine, and threonine, as well as odd-chain fatty acids.[3,4] The enzyme is composed of six α and six β subunits encoded by their respective genes, *PCCA* and *PCCB*.[5] PA is caused by variants in the *PCCA* or *PCCB* genes at equal frequencies.[2,6–9] PCC catalyzes the first step in conversion of propionyl-CoA to D-methylmalonyl-CoA in the pathway of propionyl-CoA oxidation, depicted in (Figure 1). PCC deficiency leads to an increase in the levels of propionyl-CoA-derived metabolites, including 2-methylcitrate,[10] propionylcarnitine,[11] and 3-hydroxypropionate,[12] which have been used as metabolic biomarkers of PA to identify patients on newborn screening, for clinical monitoring, and in genomic therapy studies.[13–15]

Most frequently, patients with PA present in the neonatal period with a life-threatening metabolic crisis, characterized by vomiting, poor feeding, hypotonia, ketoacidosis, and hyperammonemia.[16] Those who survive suffer from recurrent metabolic instability and can develop multisystemic complications, which can include cardiomyopathy.[17,18] Over the decades, it has been recurrently documented that PA patients with an early and severe clinical course experience increased mortality and disease-associated morbidity.[2,19,20] The recalcitrant nature of the disorder to conventional medical management, including dietary restriction of amino acid precursors, L-carnitine supplementation, and administration of metronidazole to reduce generation of propionic acid by intestinal bacteria, has led to implementation of elective liver transplantation (LT) as an experimental surgical treatment for PA.[21–23] While not curative of all aspects of this disorder, successful LT in the setting of PA provides restoration of metabolic stability and protection from early death and therefore represents a clinical benchmark for gene replacement or addition approaches that might increase hepatic PCC expression and activity.[22] Whether an LT is protective against development of cardiomyopathy in PA is unknown but seems unlikely, given the recent reports describing progression of cardiac disease after successful LT, leading to death in one reported patient and the need for a heart transplant in another,[24,25] highlighting the need for therapies that target extrahepatic organs.

Received 5 January 2023; accepted 21 June 2023;
https://doi.org/10.1016/j.omtm.2023.06.008.

Correspondence: Charles P. Venditti MD, PhD, Organic Acid Research Section, Metabolic Medicine Branch, National Human Genome Research Institute, National Institutes of Health, Bldg. 10, Room 7N248A, Bethesda, MD 20892, USA.
E-mail: venditti@mail.nih.gov

This is an open access article under the CC BY-NC-ND license (http://creativecommons.org/licenses/by-nc-nd/4.0/).

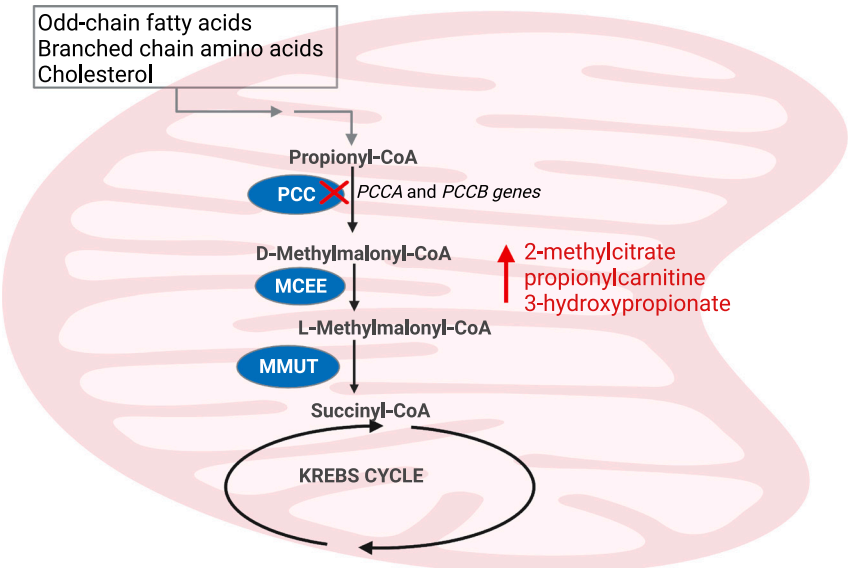

Figure 1. Mitochondrial catabolism of propionyl-CoA to succinyl-CoA

Propionic acidemia (PA) is caused by mutations in the *PCCA* or *PCCB* gene, which encode for the respective subunits of propionyl-CoA carboxylase (PCC). Enzymes downstream of PCC in the metabolism of propionyl-CoA to succinyl-CoA, a Krebs cycle intermediate. Other enzymes include D-methylmalonyl-CoA epimerase (MCEE) and methylmalonyl-CoA mutase (MMUT). The figure was created with BioRender.

Over the past decade, adenovirus- and adeno-associated virus (AAV)-based gene therapies have been studied in mouse models of PCCA deficiency, with variable success.[13,14,19,26] The mouse models used in these studies were made either by creating a large genomic deletion in the *Pcca* gene or through overexpression of a hypomorphic *PCCA* allele as a germline transgene under control of a strong heterologous enhancer/promoter.[14,27] Here, we used genome editing to create a small deletion in exon 5 of *Pcca*, resulting in a frameshift (c.398_401delAAGC p.(Gln133Leufs*41)), similar to the type of variants that occur in some PA patients.[28] Homozygous $Pcca^{c.398\_401delAAGC}$ mice, hereafter designated $Pcca^{-/-}$, recapitulate the severe neonatal presentation of PA and manifest uniform neonatal lethality, absent PCCA expression, and increased 2-methylcitrate. We next explored the utility of an AAV44.9 pseudoserotyped vector to treat $Pcca^{-/-}$ mice.[29,30] This capsid was selected because it has recently been recognized to result in pronounced hepato-cardiac transduction after systemic delivery and to treat mice with the related disorder methylmalonic acidemia (MMA).[31] Here we show that a single dose of an AAV44.9-PCCA vector, delivered by retro-orbital injection at a dose of 1e11 vg/pup, increased survival and *PCCA* mRNA and PCCA protein levels and reduced plasma 2-methylcitrate levels in treated PA mice. Of note, there was enhanced transduction and robust transgene expression in the hearts of the treated $Pcca^{-/-}$ mice, which suggests that AAV44.9 vectors, in addition to restoring hepatic PCC activity, might be useful to treat cardiomyopathy, a common and often lethal complication of PA.

RESULTS

Creation and characterization of a new *Pcca* allele

CRISPR-Cas9 genome editing was used to engineer a frameshift-stop mutation in the *Pcca* gene. A CRISPR guide RNA was designed to target the biotin carboxylation domain of the PCCA subunit, and co-injected with *Cas9* mRNA were into zygotes, resulting in a 4-bp deletion in exon 5 of the *Pcca* gene after cleavage and non-homologous end joining (Figure 2). The corresponding variant, $Pcca^{c.398\_401delAAGC}$, is predicted to result in the truncated and non-functional protein PCCA $^{p.Gln133Leufs*41}$ (Figure S1).

$Pcca^{-/-}$ mice display a severe neonatal-lethal phenotype (Figure 3A). At birth, these mice are indistinguishable from their phenotypically wild-type littermates ($Pcca^{+/+}$ and $Pcca^{+/-}$) but have significantly decreased survival ($p < 0.001$, log rank [Mantel-Cox] test), uniformly perishing within the first 2 days of life. $Pcca^{+/+}$, $Pcca^{+/-}$, and $Pcca^{-/-}$ mice were culled on day of life 1 to examine metabolic changes and *Pcca* expression. $Pcca^{-/-}$ newborn pups had significantly elevated plasma 2-methylcitrate (Figure 3B) in comparison with their wild-type newborn littermates ($Pcca^{-/-}$ = 37.89 ± 1.35 μM versus wild type [WT] = 0.62 ± 0.02 μM, Mann-Whitney test, $p < 0.001$). Total RNA was extracted from the liver of the pups, and qRT-PCR was performed to access the relative transcriptional level to the endogenous murine *Pcca* mRNA with normalization to β-actin (*Actb*) mRNA. $Pcca^{+/-}$ and $Pcca^{-/-}$ mice had significantly lower levels *Pcca* mRNA expression than $Pcca^{+/+}$ mice (Figure 3C), with mean levels of *Pcca* mRNA of 56.3% ± 3.8% ($p < 0.001$, one-way ANOVA) and 11.3% ± 0.3% ($p < 0.001$, one-way ANOVA), respectively. $Pcca^{-/-}$ mice also had significantly lower levels of *Pcca* mRNA expression than $Pcca^{+/-}$ mice ($p < 0.01$, one-way ANOVA). Immunoblotting of liver tissue lysates from $Pcca^{-/-}$ newborn pups with an anti-PCCA antibody failed to detect PCCA protein relative to their phenotypically normal littermates (Figure 3D). While the levels of endogenous PCCA in the livers of $Pcca^{+/-}$ mice appeared to be lower than the PCCA levels in $Pcca^{+/+}$ mice, this difference was not significant (Figure S2). Hepatic lipidosis was the only histopathology finding in newborn $Pcca^{-/-}$ pups (Figure S3A). Notably, the heart was grossly and microscopically without abnormalities (Figure S3B).

Treatment with an AAV44.9 vector increases the survival of $Pcca^{-/-}$ mice and decreases a disease-related biomarker

A previously described AAV PCCA transgene, pAAV-CBA-PCCA, was pseudotyped with an AAV44.9 capsid to create AAV44.9-CBA-PCCA (Figure 4A).[13] $Pcca^{-/-}$ mice were injected via the retro-orbital route on the first day of life with either 1e10 vg or 1e11 vg of

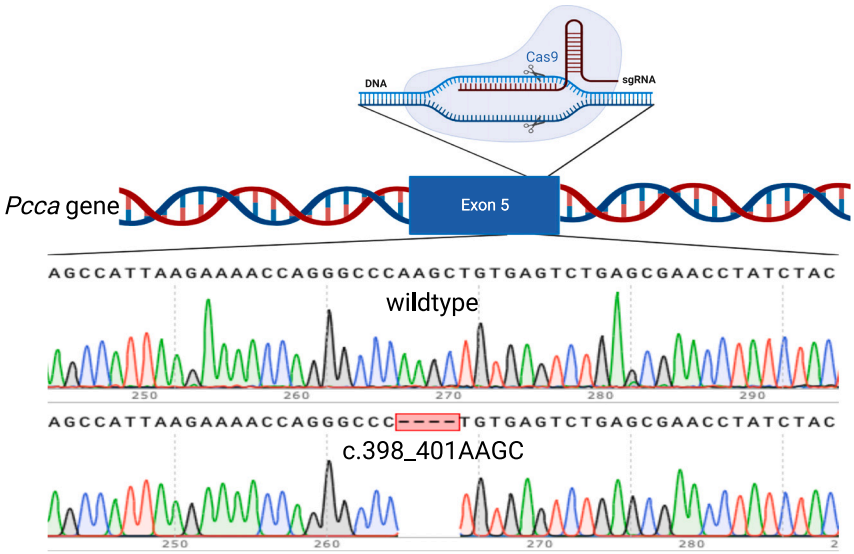

Figure 2. Schematic of the *Pcca*$^{c.398\_401delAAGC}$ allele
Exon 5 of the *Pcca* was targeted with a single-guide RNA (sgRNA) resulting in a 4-bp deletion after Cas9 cleavage and repair by non-homologous end joining (NEHJ). Shown are Sanger sequencing results of genomic DNA from a mouse with a WT *Pcca* genotype compared with a mouse homozygous for the *Pcca*$^{c.398\_401delAAGC}$ mutation (bottom). The figure was created with BioRender.

AAV44.9-CBA-PCCA. The mice treated with a dose of 1e11 vg had a significant increase in survival (Mantel-Cox test, p = 0.003), with a few treated mice surviving longer than 150 days (Figure 4B). By comparison, *Pcca*$^{-/-}$ mice that were treated with a dose of 1e10 vg or left untreated did not survive more than 2 days. The AAV44.9-CBA-PCCA-treated *Pcca*$^{-/-}$ mice that survived were smaller than their WT littermates (Figure S4) and appeared otherwise healthy but slowly declined, with ruffled coats, hunching, and progressive lethargy. The cause(s) of demise in the mice was/were undetermined, with most animals found dead and unsuitable for further study. Gross examination of the deceased mice that were studied before autolysis was unremarkable, with no obvious changes in the size or appearance of the internal organs. 4 days (n = 3) and 1–3 months (n = 14) post treatment, the AAV44.9-CBA-PCCA-treated *Pcca*$^{-/-}$ mice had significantly reduced mean plasma 2-methylcitrate levels (p = 0.002 and 0.02, respectively; one-way ANOVA) of 32.7 ± 5.1 μM in comparison with untreated newborn *Pcca*$^{-/-}$ pups (n = 13), which had a mean of level of 45.1 ± 2.1 μM (Figure 4C). However, 2-methylcitrate levels in treated *Pcca*$^{-/-}$ mice remained elevated in comparison with *Pcca*$^{+/+}$ mice (n = 5) at 1 month of age, which had a mean level of 0.56 ± 0.21 μM.

Vector biodistribution, PCCA mRNA expression, and PCCA protein transgene expression

Three AAV44.9 treated *Pcca*$^{-/-}$ mice were sacrificed at 4 days and 1 month post treatment to determine the biodistribution of the vector and the expression of mRNA and protein from the AAV transgene. Vector copy number in the liver, heart, skeletal muscle, brain, and kidneys was determined using digital droplet PCR (ddPCR) to detect the *PCCA* transgene and the murine *Gapdh* gene and is reported as a ratio of the copy number of *PCCA* to *Gapdh* (Figure 4D). *Pcca*$^{-/-}$ mice on day 4 post treatment had mean vector copies in the heart (29.04 ± 7.65, n = 3) and liver (28.53 ± 8.22, n = 3). The ratio of *PCCA*/*Gapdh* 30 days post treatment was highest in the heart (3.7 ± 0.6, n = 3) in comparison with the liver (2.2 ± 0.7, n = 3), and both ratios were significantly higher than in skeletal muscle, brain, and kidneys, which all had mean values of less than 0.5 *PCCA*/*Gapdh*. Transgene mRNA expression in AAV44.9-treated *Pcca*$^{-/-}$ mice 30 days post treatment and untreated controls was determined using probes specific to *PCCA*, *Actb* (liver), *Gapdh* (heart), and endogenous *Pcca*. *PCCA* mRNA was detectable by qRT-PCR 1 month post treatment in the livers and hearts of AAV44.9-treated *Pcca*$^{-/-}$ mice at levels of approximately 4% and 160% that of WT endogenous *Pcca* RNA expression (Figure 4E). Low levels of a *Pcca* transcript were detectable in the livers and hearts of untreated *Pcca*$^{-/-}$ mice at approximately 10%–15% of the levels seen in WT mice, and no *PCCA* transgene mRNA signal was detected in untreated control mice. Immunoblotting with an antibody capable of detecting the endogenous murine and the human PCCA protein was used to determine PCCA expression at 4 days (Figure 5A) and 1 month post treatment with a retro-orbital sinus injection on day of life 1 with 1e11 vg of AAV44.9. While no PCCA expression was detected in untreated *Pcca*$^{-/-}$ mice, AAV44.9-treated *Pcca*$^{-/-}$ mice 4 days post treatment were determined to have 68.5% ± 24.4% (n = 3) and 352.4% ± 92.6.0% (n = 2) of WT (*Pcca*$^{+/+}$) PCCA protein levels in the liver and heart, respectively (Figures 5A and 5C). Interestingly, PCCA protein expression in the liver of a single treated AAV44.9 *Pcca*$^{+/-}$ mouse 4 days after treatment was higher than the PCCA protein expression in the liver of an untreated *Pcca*$^{+/-}$ mouse (Figure 5A) but less than that seen in the treated *Pcca*$^{-/-}$ mice. By 30 days post treatment, AAV44.9-treated *Pcca*$^{-/-}$ mice had decreased levels of relative PCCA protein of 49.7% ± 4.4% and 214% ± 19.0% in the liver (n = 3) and heart (n = 3), respectively (Figures 5D and 5C).

RNA *in situ* hybridization to detect PCCA in the liver, heart, skeletal muscle, brain, and kidneys

A hybridization probe was designed specifically to detect the human *PCCA* mRNA expressed by the AAV vector transgene and not to cross-react with endogenous murine transcripts. *PCCA* mRNA was detected (punctate red staining) in the liver, heart, and skeletal muscle and variably in the brain but not in the kidneys 1 month post treatment (Figure 6). The greatest amount of *PCCA* mRNA was observed in the heart. Smaller numbers of positively stained cells were also seen in the liver and skeletal muscle. The distribution of *PCCA* RNA-positive cells was uniform in the heart, liver, and skeletal muscle. While two of the three AAV44.9-treated mice had minimal positive staining

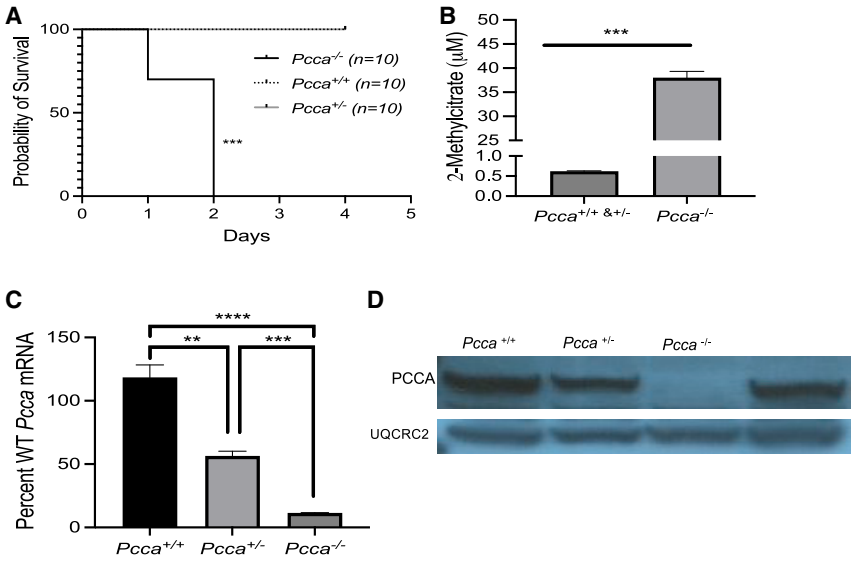

Figure 3. Clinical and biochemical characterization of *Pcca*$^{-/-}$ mice

(A) Survival of mice with *Pcca*$^{+/+}$, *Pcca*$^{+/-}$, and a *Pcca*$^{-/-}$ genotypes. (B) Plasma 2-methylcitrate levels from *Pcca*$^{+/+}$ and *Pcca*$^{+/-}$ newborn pups (n = 13) in comparison with *Pcca*$^{-/-}$ newborn pups (n = 6). (C) *Pcca* mRNA levels in the liver of *Pcca*$^{+/+}$ (n = 3), *Pcca*$^{+/-}$ (n = 3), and *Pcca*$^{-/-}$ (n = 3) mice, shown as a percentage of WT *Pcca* mRNA expression normalized to *Actb*. (D) Immunoblot of 50 μg hepatic protein from *Pcca*$^{+/+}$, *Pcca*$^{+/-}$, and *Pcca*$^{-/-}$ newborn pups for the PCCA protein using the mitochondrial protein ubiquinol-cytochrome *c* reductase core protein 2 (UQCRC2) as a loading control. **p < 0.01, ***p < 0.001, ****p < 0.0001.

in the brain, a single mouse had a localized area with many positively stained cells (Figure 6C).

DISCUSSION

PA was first recognized as a human inborn error of metabolism in the 1960s, and the clinical presentation of severe patients has remained unchanged for many decades, with a neonatal metabolic crisis still typical as the first manifestation of illness, even in an era of newborn screening.[32] While early recognition of PA and related organic acidemias during infancy has undoubtably led to improved diagnosis and a more rapid implementation of supportive therapies, such as hemodialysis, the outcomes for patients remain guarded.[2] The difficult clinical course many patients experience has led to implementation of elective LT as a surgical treatment for PA, providing a strong rationale for development of alternative therapies.[33–36]

As part of an effort to develop AAV gene therapy for PA, we critically assessed the current animal models to inform our approach. The first mouse model of PA was generated by targeted disruption of the *Pcca* gene via homologous recombination in embryonic stem cells.[27] The mutant allele, *Pcca*^{del}, contains a several-kilobase-pair deletion in *cis* with a neomycin cassette and replaces exons 1–4 of the *Pcca* gene. *Pcca*$^{del/del}$ mice perish within the first 48 hours after birth and lack PCCA expression. The earliest gene therapy studies using these mice yielded disappointing results; treatment with an adenoviral vector designed to express the human PCCA cDNA produced an increase in life expectancy of only several hours, with AAV serotype 8 (AAV8)-mediated gene transfer of PCCA equally ineffective.[26] However, a later study of the very same *Pcca*$^{del/del}$ mice, informed by a series of successful experiments with mouse models of MMA, demonstrated that systemic delivery of a reconfigured AAV8 vector that expressed the human *PCCA* gene under control of a strong heterologous promoter provided effective rescue from neonatal lethality, restoration of hepatic PCC expression, and a substantial reduction in the plasma level of the associated biomarker, 2-methylcitrate.[13,37–39] Despite successful rescue with an improved AAV8 vector, the fragility of the *Pcca*$^{del/del}$ mice led Guenzel et al.[14,19,40] to develop transgenic mice that overexpress a human mutation, PCCA$^{p.A138T}$, under control of the hybrid cytomegalovirus early enhancer/chicken β-actin (CAG) promoter. Breeding to create *Pcca*$^{del/del}$ Tg$^{CAG\text{-}PCCA(p.A138T)IRES\text{-}GFP}$ mice yielded a hypomorphic mouse model of PA. *Pcca*$^{del/del}$ Tg$^{CAG\text{-}PCCA(p.A138T)IRES\text{-}GFP}$ mice are rescued from severe PA by expression of PCCA$^{p.A138T}$ and are mildly affected, displaying preserved survival into the adult period and only modest elevations of biochemical markers of the disease.[14] Even though this model does not recapitulate the most salient clinical features of PA, specifically early lethality, *Pcca*$^{del/del}$ Tg$^{CAG\text{-}PCCA(p.A138T)IRES\text{-}GFP}$ mice have been used to test adenoviral and AAV8, AAV1, and AAVrh10 PCCA vectors, all of which variably reduce the levels of metabolites after gene delivery.[14,19,40] An additional limitation of this model is that the rescue transgene does not uniformly express PCCA$^{p.A138T}$ in different tissues and between sexes. Indeed, Subramanian et al.[41] noted that there was highly disparate PCCA$^{p.A138T}$ expression in *Pcca*$^{del/del}$ Tg$^{CAG\text{-}PCCA(p.A138T)IRES\text{-}GFP}$ mice that did not correlate with the endogenous levels of PCCA, indicating that the rescue transgene is susceptible to epigenic effects or that overexpression of the mutant protein may have other untoward effects, such as interference with formation of a stable PCC heterododecamer. The gaps between the PA models and clinically relevant patient phenotypes led us to create a new *Pcca* allele, which was then used in a proof-of-concept study with a novel AAV capsid.

Because a majority of the PA patients have small deletions, insertions, and missense mutations in the *PCCA* gene, and the existing *Pcca*$^{del/del}$ Tg$^{CAG\text{-}PCCA(p.A138T)IRES\text{-}GFP}$ model does not recapitulate the severe clinical phenotype of PA seen in many patients, especially those who might benefit from AAV gene therapy, we used genome editing to engineer a 4-bp deletion, causing a frameshift mutation (*Pcca* c.398_401delAAGC).[6] *Pcca*$^{-/-}$ (c.398_401delAAGC) mice have a severe neonatal lethal phenotype and elevated plasma 2-methylcitrate and lack PCCA protein. Interestingly, *Pcca*$^{+/-}$ (c.398_401delAAGC) mice express less *PCCA* mRNA than *Pcca*$^{+/+}$ mice but have similar

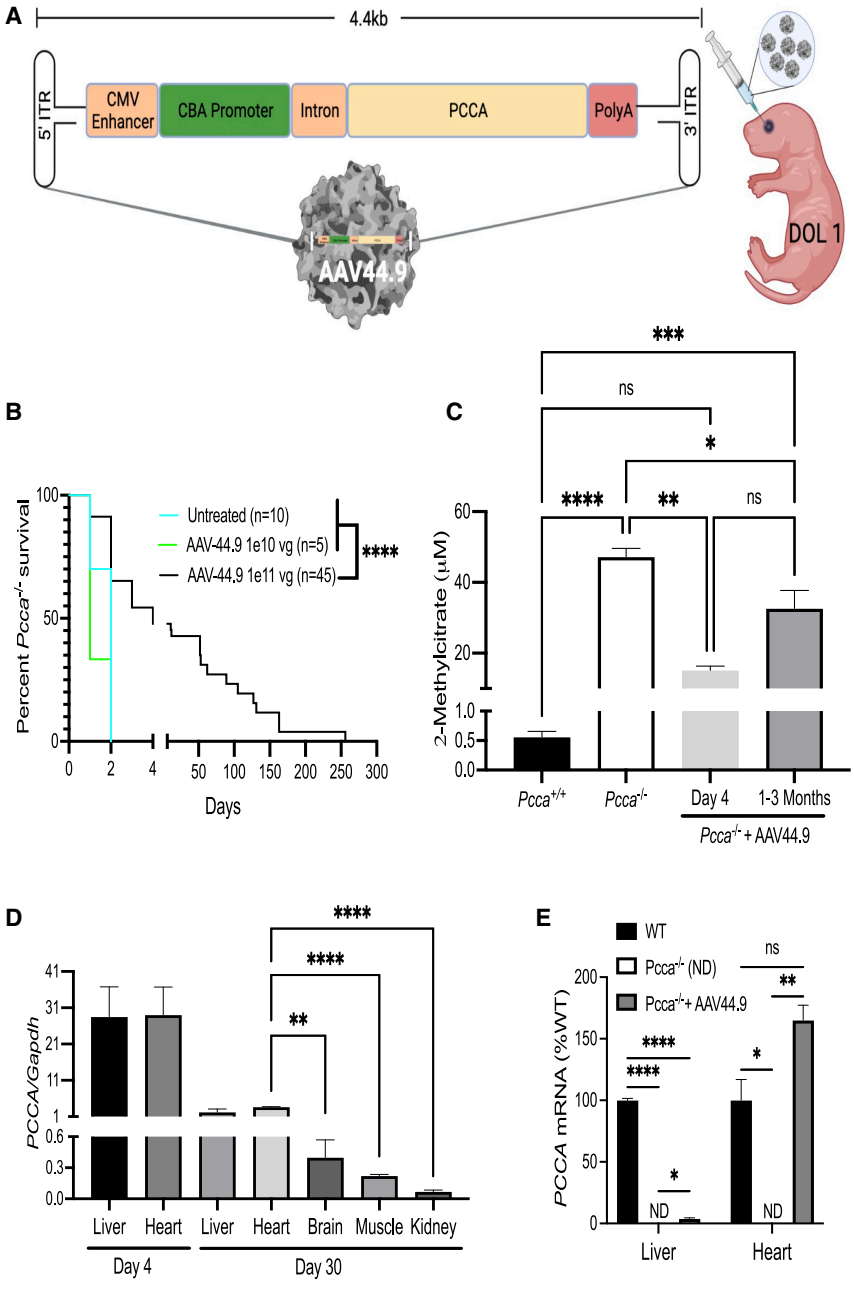

Figure 4. AAV44.9 gene delivery of PCCA rescues *Pcca*$^{-/-}$ mice from neonatal lethality

(A) Schematic of the recombinant AAV vector genome (pAAV-CBA-PCCA) packaged with the AAV44.9 capsid (CMV, cytomegalovirus; CBA, chicken β-actin). *Pcca*$^{-/-}$ pups received a retro-orbital injection of 1e10 vg or 1e11 vg of AAV44.9-CBA-PCCA on day of life 1 (DOL 1). (B) Survival curve comparing the viability of *Pcca*$^{-/-}$ mice treated with AAV44.9 at doses of 1e10 vg or 1e11 vg with untreated *Pcca*$^{-/-}$ mice. (C) Plasma 2-methylcitrate in untreated neonatal *Pcca*$^{-/-}$ mice and *Pcca*$^{-/-}$ mice 4 days and 1–3 months after treatment with AAV44.9 at 1e11 vg. (D) Vector biodistribution in liver, heart, brain skeletal muscle, and kidneys from *Pcca*$^{-/-}$ treated mice (n = 3) 4 days and 1 month post treatment, as determined by ddPCR. (E) *PCCA* and *Pcca* mRNA expression in the liver and heart (WT, n = 3, 3; PA, n = 2, 1; AAV44.9, n = 3, 3), shown as a percentage of WT *Pcca* mRNA expression normalized to *Actb* (liver) or *Gapdh* (heart). *p < 0.05, **p < 0.01, ***p < 0.001, ****p < 0.0001; ns, not significant; ND, not detected.

levels of PCCA protein. As with carriers of *PCCA* variants in humans, heterozygous mice do not have elevated plasma 2-methylcitrate or display any phenotypes associated with PA.

The multisystemic presentation of PA and ubiquitous expression of the PCC enzyme led to the design of a vector transgene with a constitutive promoter to test AAV gene therapy and the *in vivo* potency of the AAV44.9 capsid. A previous study that examined systemic gene delivery in a mouse model of the related disorder MMA reported that AAV44.9 was highly efficient at transducing the liver and heart,[31] targets for transgene expression in patients with PA. Indeed, AAV44.9-treated *Pcca*$^{-/-}$ (c.398_401delAAGC) mice had significantly improved survival and reduced 2-methylcitrate, a disease biomarker. Transduction and transgene expression were detected in multiple tissue types that included the liver, heart, skeletal muscle, and brain. The heart had the highest level transgene expression, followed by the liver. Unfortunately, most of the rescued PA mice died between 1 and 3 months of age, likely because of loss of the episomal AAV vector, a well recognized outcome that follows AAV delivery to neonatal animals.[42,43] To date, only AAV44.9 and AAV8 gene delivery have been potent enough to rescue neonatal lethal models of PA, which is important because patients with early and severe presentation of PA have the greatest need for new therapies, and these AAV capsids likely have distinct seroreactivity in humans.[31]

The AAV44.9 capsid enabled widespread transduction and transgene expression in PA mice. *In situ* hybridization detected cells expressing *PCCA* mRNA in the liver, heart, skeletal muscle, and brain at levels consistent with the vector transgene in the respective tissues. The distribution of cells expressing the transgene appeared to be homogeneous except for the brain, where positively stained cells were localized in the forebrain. While two of the AAV44.9-treated mice studied only had rare cells that expressed *PCCA*, a single mouse had a larger area of positively stained cells. That this was a consequence of an aberrant retro-orbital injection seems likely, but the overall results suggest that AAV44.9 can transduce neurons. More targeted investigations to examine the

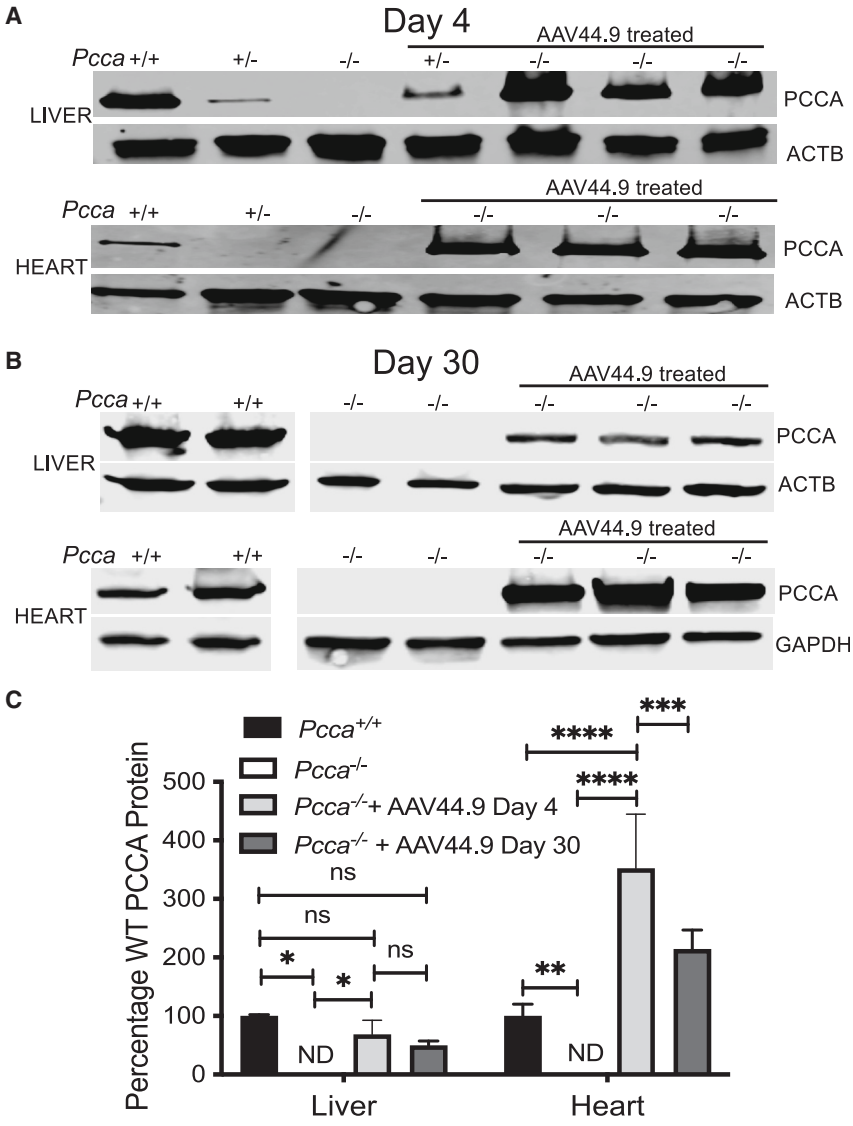

Figure 5. Expression of PCCA protein in the liver and heart

(A) Immunoblot of hepatic and cardiac PCCA protein from untreated *Pcca*$^{+/+}$ (n = 1), *Pcca*$^{-/-}$ (n = 1), and *Pcca*$^{+/-}$ (n = 1) and AAV44.9-treated *Pcca*$^{+/-}$ (n = 1) and *Pcca*$^{-/-}$ (n = 3) mice 4 days post treatment. (B) Immunoblot of hepatic and cardiac PCCA protein from untreated *Pcca*$^{+/+}$ (n = 2) and *Pcca*$^{-/-}$ (n = 2) and AAV44.9-treated *Pcca*$^{-/-}$ mice (n = 3) 30 days post treatment. (C) Quantification of PCCA protein expression relative to untreated *Pcca*$^{+/+}$ mice from the blots depicted in (A) and (B). *p < 0.05, **p < 0.003, ***p < 0.001, ****p < 0.0001.

specific neurotropism of AAV44.9, which was not an objective of the current study, will be necessary but seem promising.

Histological examination of the heart of untreated *Pcca*$^{-/-}$ (c.398_401delAAGC) neonatal mice in this study did not reveal any cardiac abnormalities (Figure S3). AAV44.9 treatment resulted in significant amounts of cardiac transduction and PCCA protein expression, which could be vital for treatment of the potentially lethal cardiomyopathy associated with PA. While AAV44.9-treated *Pcca*$^{-/-}$ mice had normal histology, without aged matched untreated controls it is not possible to assess the effects of gene therapy on the heart (Figure S5). Therefore, to truly measure the effects of gene therapy on the cardiomyopathy of PA, the creation of *Pcca* knockin, conditional, or tissue-specific transgenic rescue mice may be required to generate a model with a consistent cardiac phenotype that replicates the human condition.

In conclusion, a new murine model of severe PA caused by PCCA deficiency has been created and characterized. The mutation is similar to those seen in patients and might be amenable to treatments using other forms of genomic therapy, such as prime editing.[44] Use of an AAV44.9 vector resulted in striking clinical and biochemical improvements in these severely affected PA mice, with robust transduction of the heart, an important target organ for treatment of PA because severe cardiomyopathy can develop in PA patients, even after LT.[24,25] Pseudoserotyped AAV44.9 vectors might therefore be especially well suited for treatment of other metabolic disorders like PA, where hepatic and cardiac targeting is needed, such as glycogen storage disorders and fatty acid oxidation defects.

MATERIALS AND METHODS

Animal studies

Animal work was approved by and performed in accordance with the guidelines for animal care at the National Institutes of Health and the Guide for the Care and Use of Laboratory Animals. All mice were housed in micro-isolators maintained under a 12-h light/12-h dark cycle. Mice were maintained on standard mouse chow (PicoLab Mouse Diet 20, LabDiet, St. Louis, MO, USA) and water, which was available *ad libitum*. Heterozygous carriers of the *Pcca* mutation were bred to generate *Pcca*$^{+/-}$ and *Pcca*$^{-/-}$ mice.

Generation of a murine model of PA caused by PCCA deficiency using CRISPR-Cas9 genome editing

DESKGEN software was used to identify protospacer-adjacent motif (PAM) sequences (NGG) from *Streptococcus pyogenes* (SpyCas9) targeting exon 5 of the *Pcca* gene for mutagenesis. A synthetic single-guide RNA (sgRNA) was custom synthesized by Horizon Discovery (Edit-R predesigned synthetic sgRNA). Zygotes were co-injected with the Cas9 mRNA and sgRNA and cultured at 37°C under 5% CO_2 until the blastocyst stage and then transferred into the uterus of pseudo-pregnant females.

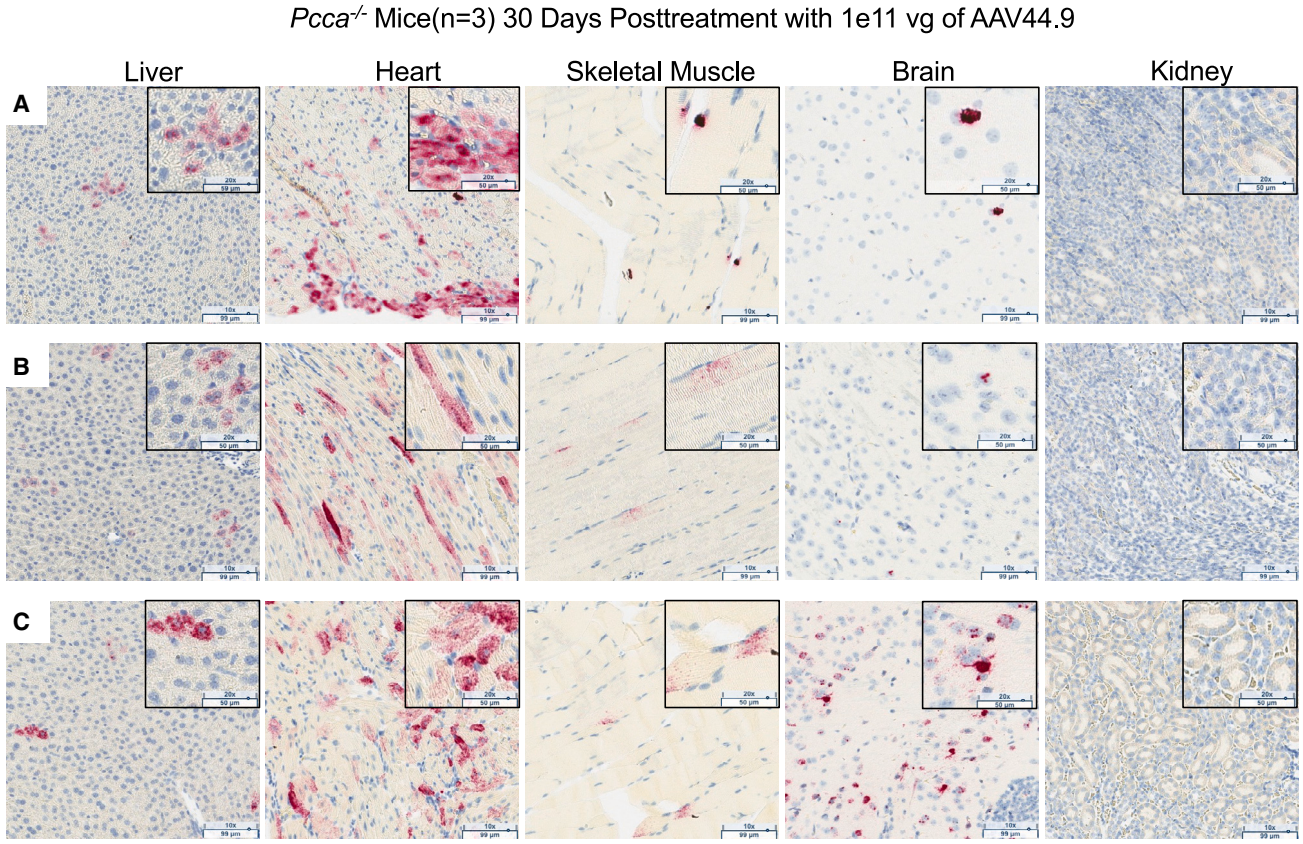

Figure 6. RNA *in situ* hybridization in tissues 30 days after AAV44.9 gene delivery to detect *PCCA* expression

PCCA transgene mRNA (punctate red staining) *in situ* hybridization (magnification, 10× with 20× inset) of liver, heart, skeletal muscle, brain, and kidney tissue from three $Pcca^{-/-}$ AAV44.9-CBA-PCCA-treated mice, labeled A, B, and C.

The *Pcca* exon5 sgRNA sequence used was : 5′-GTTCGCTCAGACT CACAGCT-3′ PAM-TGG.

Founder and colony genotyping

DNA was extracted from tail clips using the DNeasy Blood & Tissue Kit (QIAGEN, Hilden, Germany) for PCR amplification. DNA samples from founders were screened using flourescent PCR (fPCR) for gene knockout using primers (*Pcca* E5_fPCRFor, *Pcca* E5_fPCRRev) that spanned exon 5 of the *Pcca* gene and crossed with WT FvBN mice to generate heterozygous carriers of the mutation, which were further bred to generate $Pcca^{-/-}$ mice. The sequence of the mutation was determined by targeted PCR of genomic DNA and Sanger sequencing using primers (*Pcca* E5for, *Pcca* E5rev) that flanked exon 5 of the *Pcca* gene. After confirmation of the genetic mutation, genotyping of tail snip lysate by qPCR was performed by Transnetyx. The qPCR primers and probes were as follows:

Pcca E5_fPCRfor, 5′-TGTAAAACGACGGCCAGTGAGCATCTGT TAATACAGGG-3′

Pcca E5_fPCRrev, 5′-GTGTCTTAACTCCAGCTTTCTGCTC-3′

Pcca E5for, 5′-AGTCACGGGTGATGCTGACC-3′

Pcca E5rev, 5′-CCTGAACTGAAGCTGCTC-3′

qPCR *Pcca* for, 5′-CTACCTCAACATGGATGCCATCAT-3′

qPCR *Pcca* rev, 5′-CATATGAAACAGCIGCAGTAGATAGGT-3′

qPCR reporter 1, 5′-TCACAGCTTGGGCCCT-3′

qPCR reporter 2, 5′-AGACTCACAGGGCCCT-3′

Metabolic measurements

Blood samples were collected using retro-orbital sinus plexus sampling with sterile heparinized glass capillary tubes. Samples were immediately centrifuged, and plasma was collected, diluted in water, and frozen at −80°C until measurements were performed. Plasma 2-methylcitrate levels were quantified by gas chromatography-mass spectrometry with stable isotopic internal calibration as described previously.[45,46]

rAAV44.9 construction, production, and delivery

The viral construct pAAV2.CB7.CI.RBG was graciously provided by the University of Pennsylvania Vector Core (Philadelphia, PA, USA), and a full-length human PCCA cDNA was cloned into this vector as described previously.[13] Production and purification of recombinant AAV44.9 were performed using a four-plasmid (AAV44.9) procedure as described previously.[30,31] Retro-orbital injections were performed on non-anesthetized neonatal mice, typically within several hours after birth. In treated litters, all pups were injected without genotyping. Viral particles were diluted to a total volume of 40 μL with phosphate-buffered saline immediately before injection.

Titration of AAVs

AAV44.9-CBA-PCCA titer was determined by quantitative real-time PCR analysis with TaqMan gene expression assays (human PCC [Hs01120571_m1]; Applied Biosystems, Foster City, CA, USA).

Vector genome quantification by ddPCR

Genomic DNA from tissue samples was extracted using the DNeasy Blood & Tissue Kit (catalog number 69506; QIAGEN). ddPCR was performed according to the manufacturer's recommendations using a Bio-Rad (Hercules, CA, USA) QX200 AutoDG ddPCR system with the following probes: Bio-Rad ddPCR copy number variation (CNV) assay *Gapdh* (assay ID dMumCNS300520369) and *PCCA* (assay ID dHsaCPE5056812).

Relative *PCCA* mRNA expression

Total RNA was extracted using RNeasy Mini with DNase digestion using the RNase-Free DNase Set (catalog numbers 74804 and 79254, QIAGEN). A cDNA library was prepared using the High-Capacity cDNA Reverse Transcription Kit with RNase Inhibitor (catalog number 4374966, Applied Biosystems). TaqMan gene expression assays for human *PCCA*, murine *Pcca*, and murine *Actb* and *Gapdh* (assay IDs Hs00165407_m1, Mm00454899_m1, and Mm00607939_s1 for liver and Mm99999915_g1 for heart, respectively; Applied Biosystems) were performed on an CFX96 Real-Time System (Bio-Rad). The gene expression assays use primers specific to the mouse Pcca and human PCCA mRNA. Quantification of relative gene expression, presented as percentage of the relevant baseline (WT), was calculated using the 2^-[delta][delta]Cq (quantification cycle) method.

PCCA mRNA *in situ* hybridization

Liver, heart, brain, kidney, and skeletal muscle tissues were fixed in 4% paraformaldehyde and embedded in paraffin blocks. Five-micrometer sections were cut and stained with the RNAScope 2.5 HD Assay-Brown (322300; ACDBio, Newark, CA, USA), following the manufacturer's instructions. Slide images were captured using the Carl Zeiss AxioScan Z1 slide scanner and analyzed using Image Pro Premier 3D v.9.3 (Media Cybernetics).

Immunoblot analysis

Previously snap-frozen livers and hearts were homogenized in of Tissue Protein Extraction Reagent (catalog number 78510; Thermo Scientific, Waltham, MA, USA) with cOmplete Tablets, Mini EDTA-free (catalog number 04693159001, Roche, Indianapolis, IN, USA). Protein concentrations were determined using a Protein Assay Dye Reagent Concentrate (catalog number 5000006; Bio-Rad) according to the manufacturer's protocol. A total of 50 μg of total protein was separate by gel electrophoresis using the Mini-PROTEAN Tetra Vertical Electrophoresis Cell with Mini-PROTEAN TGX Gels (catalog numbers 1658004 and 4561084, Bio-Rad, respectively). Protein transfer was accomplished using a Trans-Blot Turbo Transfer Pack (catalog number 1704156, Bio-Rad). EveryBlot Blocking Buffer (catalog number 12010020, Bio-Rad) was used for blocking and antibody hybridization. The following antibodies were used for detection of PCCA (Abcam, ab187686) at a dilution of 1:1,000; UQCRC2 (Abcam, ab14745) at a dilution of 1:2,000; GAPDH (Proteintech, catalog number 60004-1-Ig) at a dilution of 1:10,000; and β-actin (Proteintech, 66009-1-Ig) at a dilution of 1:10,000 in conjunction with the following secondary antibodies at a dilution of 1:20,000: (LI-COR Biosciences, 926-32213) and (LI-COR Biosciences, 926-68072). Blots were imaged using the LI-COR Biosciences Odyssey DLx imaging system and LI-COR Biosciences acquisition software.

Statistical analyses

Prism 9 v.9.2.0 (GraphPad) was used to analyze all data. Results are expressed as mean ± SD. Values of $p < 0.05$ were considered statistically significant. Depending on the experimental design, Mann-Whitney test, a one-way ANOVA, or log rank (Mantel-Cox) test were used to test for statistical significance, and the test used is specified under Results.

DATA AND CODE AVAILABILITY

Data supporting the studies presented in this manuscript can be made available by request to the corresponding authors.

SUPPLEMENTAL INFORMATION

Supplemental information can be found online at https://doi.org/10.1016/j.omtm.2023.06.008.

ACKNOWLEDGMENTS

We appreciate the assistance of the NHGRI mouse core, especially Gene Elliot and Cecilia Rivas; the NCI Molecular Pathology Lab, especially Andrew Warner; and Darwin Romero for help with treating animals and collecting murine tissues. R.J.C., D.C., E.-Y.C., L.L., S.N.S., J.L.S., and C.P.V. were supported by the Intramural Research Program of the NHGRI through 1ZIAHG200318-16. C.P.V. also acknowledges support from the National Center for Advancing Translational Sciences (NCATS) and the Organic Acid Association. G.D.P. and J.A.C. were supported by the Intramural Research Program of the NIDCR through Z01 DE00695.

AUTHOR CONTRIBUTIONS

R.J.C., conceptualization, methodology, validation, formal analysis, investigation, data curation, writing (first draft, review and editing), visualization, and project administration; C.P.V. and J.A.C., conceptualization, writing (review and editing), funding acquisition, and

project administration; G.D.P., D.C., E.-Y.C., S.N.S., J.L.S., V.H., and L.L., formal analysis, investigation, and writing (review and editing).

DECLARATION OF INTERESTS

R.J.C., G.D.P., J.A.C., and C.P.V. are inventors on a patent application filed by the NIH on their behalf on use of AAV44.9 as a gene therapy vector to treat methylmalonic acidemia.

REFERENCES

1. Almási, T., Guey, L.T., Lukacs, C., Csetneki, K., Vokó, Z., and Zelei, T. (2019). Systematic literature review and meta-analysis on the epidemiology of propionic acidemia. Orphanet J. Rare Dis. *14*, 40. https://doi.org/10.1186/s13023-018-0987-z.
2. Shchelochkov, O.A., Carrillo, N., and Venditti, C. (1993). Propionic Acidemia. In GeneReviews((R)), M.P. Adam, D.B. Everman, G.M. Mirzaa, R.A. Pagon, S.E. Wallace, L.J.H. Bean, K.W. Gripp, and A. Amemiya, eds.
3. Gompertz, D., Storrs, C.N., Bau, D.C., Peters, T.J., and Hughes, E.A. (1970). Localisation of enzymic defect in propionicacidaemia. Lancet *1*, 1140–1143. https://doi.org/10.1016/s0140-6736(70)91216-x.
4. Hsia, Y.E., Scully, K.J., and Rosenberg, L.E. (1971). Inherited propionyl-Coa carboxylase deficiency in "ketotic hyperglycinemia". J. Clin. Invest. *50*, 127–130. https://doi.org/10.1172/JCI106466.
5. Huang, C.S., Sadre-Bazzaz, K., Shen, Y., Deng, B., Zhou, Z.H., and Tong, L. (2010). Crystal structure of the alpha(6)beta(6) holoenzyme of propionyl-coenzyme A carboxylase. Nature *466*, 1001–1005. https://doi.org/10.1038/nature09302.
6. Desviat, L.R., Pérez, B., Pérez-Cerdá, C., Rodríguez-Pombo, P., Clavero, S., and Ugarte, M. (2004). Propionic acidemia: mutation update and functional and structural effects of the variant alleles. Mol. Genet. Metabol. *83*, 28–37. https://doi.org/10.1016/j.ymgme.2004.08.001.
7. Ma, X., Liu, Y., Chen, Z.H., Zhang, Y., Dong, H., Song, J.Q., Jin, Y., Li, M.Q., Kang, L.L., He, R.X., et al. (2022). [Phenotypes and genotypes of 78 patients with propionic acidemia]. Zhonghua Yufang Yixue Zazhi *56*, 1263–1271. https://doi.org/10.3760/cma.j.cn112150-20220620-00630.
8. Liu, Y., Chen, Z., Dong, H., Ding, Y., He, R., Kang, L., Li, D., Shen, M., Jin, Y., Zhang, Y., et al. (2022). Analysis of the relationship between phenotypes and genotypes in 60 Chinese patients with propionic acidemia: a fourteen-year experience at a tertiary hospital. Orphanet J. Rare Dis. *17*, 135. https://doi.org/10.1186/s13023-022-02271-3.
9. Ugarte, M., Perez-Cerda, C., Rodriguez-Pombo, P., Desviat, L.R., Perez, B., Richard, E., Muro, S., Campeau, E., Ohura, T., and Gravel, R.A. (1999). Overview of mutations in the PCCA and PCCB genes causing propionic acidemia. Hum. Mutat. *14*, 275–282. https://doi.org/10.1002/(SICI)1098-1004(199910)14:4<275::AID-HUMU1>3.0.CO;2-N.
10. Ando, T., Rasmussen, K., Wright, J.M., and Nyhan, W.L. (1972). Isolation and identification of methylcitrate, a major metabolic product of propionate in patients with propionic acidemia. J. Biol. Chem. *247*, 2200–2204.
11. Chace, D.H., DiPerna, J.C., Kalas, T.A., Johnson, R.W., and Naylor, E.W. (2001). Rapid diagnosis of methylmalonic and propionic acidemias: quantitative tandem mass spectrometric analysis of propionylcarnitine in filter-paper blood specimens obtained from newborns. Clin. Chem. *47*, 2040–2044.
12. la Marca, G., Malvagia, S., Pasquini, E., Innocenti, M., Donati, M.A., and Zammarchi, E. (2007). Rapid 2nd-tier test for measurement of 3-OH-propionic and methylmalonic acids on dried blood spots: reducing the false-positive rate for propionylcarnitine during expanded newborn screening by liquid chromatography-tandem mass spectrometry. Clin. Chem. *53*, 1364–1369. https://doi.org/10.1373/clinchem.2007.087775.
13. Chandler, R.J., Chandrasekaran, S., Carrillo-Carrasco, N., Senac, J.S., Hofherr, S.E., Barry, M.A., and Venditti, C.P. (2011). Adeno-associated virus serotype 8 gene transfer rescues a neonatal lethal murine model of propionic acidemia. Hum. Gene Ther. *22*, 477–481. https://doi.org/10.1089/hum.2010.164.
14. Guenzel, A.J., Hofherr, S.E., Hillestad, M., Barry, M., Weaver, E., Venezia, S., Kraus, J.P., Matern, D., and Barry, M.A. (2013). Generation of a hypomorphic model of propionic acidemia amenable to gene therapy testing. Mol. Ther. *21*, 1316–1323. https://doi.org/10.1038/mt.2013.68.
15. Jiang, L., Park, J.S., Yin, L., Laureano, R., Jacquinet, E., Yang, J., Liang, S., Frassetto, A., Zhuo, J., Yan, X., et al. (2020). Dual mRNA therapy restores metabolic function in long-term studies in mice with propionic acidemia. Nat. Commun. *11*, 5339. https://doi.org/10.1038/s41467-020-19156-3.
16. Pena, L., Franks, J., Chapman, K.A., Gropman, A., Ah Mew, N., Chakrapani, A., Island, E., MacLeod, E., Matern, D., Smith, B., et al. (2012). Natural history of propionic acidemia. Mol. Genet. Metabol. *105*, 5–9. https://doi.org/10.1016/j.ymgme.2011.09.022.
17. Baumgartner, D., Scholl-Bürgi, S., Sass, J.O., Sperl, W., Schweigmann, U., Stein, J.I., and Karall, D. (2007). Prolonged QTc intervals and decreased left ventricular contractility in patients with propionic acidemia. J. Pediatr. *150*, 192–197.e1. https://doi.org/10.1016/j.jpeds.2006.11.043.
18. North, K.N., Korson, M.S., Gopal, Y.R., Rohr, F.J., Brazelton, T.B., Waisbren, S.E., and Warman, M.L. (1995). Neonatal-onset propionic acidemia: neurologic and developmental profiles, and implications for management. J. Pediatr. *126*, 916–922. https://doi.org/10.1016/s0022-3476(95)70208-3.
19. Guenzel, A.J., Collard, R., Kraus, J.P., Matern, D., and Barry, M.A. (2015). Long-term sex-biased correction of circulating propionic acidemia disease markers by adeno-associated virus vectors. Hum. Gene Ther. *26*, 153–160. https://doi.org/10.1089/hum.2014.126.
20. van der Meer, S.B., Poggi, F., Spada, M., Bonnefont, J.P., Ogier, H., Hubert, P., Depondt, E., Rapoport, D., Rabier, D., Charpentier, C., et al. (1996). Clinical outcome and long-term management of 17 patients with propionic acidaemia. Eur. J. Pediatr. *155*, 205–210. https://doi.org/10.1007/BF01953939.
21. Charbit-Henrion, F., Lacaille, F., McKiernan, P., Girard, M., de Lonlay, P., Valayannopoulos, V., Ottolenghi, C., Chakrapani, A., Preece, M., Sharif, K., et al. (2015). Early and late complications after liver transplantation for propionic acidemia in children: a two centers study. Am. J. Transplant. *15*, 786–791. https://doi.org/10.1111/ajt.13027.
22. Curnock, R., Heaton, N.D., Vilca-Melendez, H., Dhawan, A., Hadzic, N., and Vara, R. (2020). Liver Transplantation in Children With Propionic Acidemia: Medium-Term Outcomes. Liver Transpl. *26*, 419–430. https://doi.org/10.1002/lt.25679.
23. Vara, R., Turner, C., Mundy, H., Heaton, N.D., Rela, M., Mieli-Vergani, G., Champion, M., and Hadzic, N. (2011). Liver transplantation for propionic acidemia in children. Liver Transpl. *17*, 661–667. https://doi.org/10.1002/lt.22279.
24. Berry, G.T., Blume, E.D., Wessel, A., Singh, T., Hecht, L., Marsden, D., Sahai, I., Elisofon, S., Ferguson, M., Kim, H.B., et al. (2020). The re-occurrence of cardiomyopathy in propionic acidemia after liver transplantation. JIMD Rep. *54*, 3–8. https://doi.org/10.1002/jmd2.12119.
25. Hejazi, Y., Hijazi, Z.M., Al-Saloos, H., and Omran, T.B. (2022). The re-occurrence of dilated cardiomyopathy in propionic acidemia after liver transplantation requiring heart transplant, first case from Middle East. Cardiol. Young *33*, 86–89. https://doi.org/10.1017/S104795112200035X.
26. Hofherr, S.E., Senac, J.S., Chen, C.Y., Palmer, D.J., Ng, P., and Barry, M.A. (2009). Short-term rescue of neonatal lethality in a mouse model of propionic acidemia by gene therapy. Hum. Gene Ther. *20*, 169–180. https://doi.org/10.1089/hum.2008.158.
27. Miyazaki, T., Ohura, T., Kobayashi, M., Shigematsu, Y., Yamaguchi, S., Suzuki, Y., Hata, I., Aoki, Y., Yang, X., Minjares, C., et al. (2001). Fatal propionic acidemia in mice lacking propionyl-CoA carboxylase and its rescue by postnatal, liver-specific supplementation via a transgene. J. Biol. Chem. *276*, 35995–35999. https://doi.org/10.1074/jbc.M105467200.
28. Kraus, J.P., Spector, E., Venezia, S., Estes, P., Chiang, P.W., Creadon-Swindell, G., Müllerleile, S., de Silva, L., Barth, M., Walter, M., et al. (2012). Mutation analysis in 54 propionic acidemia patients. J. Inherit. Metab. Dis. *35*, 51–63. https://doi.org/10.1007/s10545-011-9399-0.
29. Boye, S.L., Choudhury, S., Crosson, S., Di Pasquale, G., Afione, S., Mellen, R., Makal, V., Calabro, K.R., Fajardo, D., Peterson, J., et al. (2020). Novel AAV44.9-Based Vectors Display Exceptional Characteristics for Retinal Gene Therapy. Mol. Ther. *28*, 1464–1478. https://doi.org/10.1016/j.ymthe.2020.04.002.
30. Di Pasquale, G., Perez Riveros, P., Tora, M., Sheikh, T., Son, A., Teos, L., Grewe, B., Swaim, W.D., Afione, S., Zheng, C., et al. (2020). Transduction of Salivary Gland Acinar Cells with a Novel AAV Vector 44.9. Mol. Ther. Methods Clin. Dev. *19*, 459–466. https://doi.org/10.1016/j.omtm.2020.10.006.

31. Chandler, R.J., Di Pasquale, G., Sloan, J.L., McCoy, S., Hubbard, B.T., Kilts, T.M., Manoli, I., Chiorini, J.A., and Venditti, C.P. (2022). Systemic gene therapy for methylmalonic acidemia using the novel adeno-associated viral vector 44.9. Mol. Ther. Methods Clin. Dev. *27*, 61–72. https://doi.org/10.1016/j.omtm.2022.09.001.

32. Martín-Rivada, Á., Cambra Conejero, A., Martín-Hernández, E., Moráis López, A., Bélanger-Quintana, A., Cañedo Villarroya, E., Quijada-Fraile, P., Bellusci, M., Chumillas Calzada, S., Bergua Martínez, A., et al. (2022). Newborn screening for propionic, methylmalonic acidemia and vitamin B12 deficiency. Analysis of 588,793 newborns. J. Pediatr. Endocrinol. Metab. *35*, 1223–1231. https://doi.org/10.1515/jpem-2022-0340.

33. Barshes, N.R., Vanatta, J.M., Patel, A.J., Carter, B.A., O'Mahony, C.A., Karpen, S.J., and Goss, J.A. (2006). Evaluation and management of patients with propionic acidemia undergoing liver transplantation: a comprehensive review. Pediatr. Transplant. *10*, 773–781. https://doi.org/10.1111/j.1399-3046.2006.00569.x.

34. Critelli, K., McKiernan, P., Vockley, J., Mazariegos, G., Squires, R.H., Soltys, K., and Squires, J.E. (2018). Liver Transplantation for Propionic Acidemia and Methylmalonic Acidemia: Perioperative Management and Clinical Outcomes. Liver Transpl. *24*, 1260–1270. https://doi.org/10.1002/lt.25304.

35. Molema, F., Martinelli, D., Hörster, F., Kölker, S., Tangeraas, T., de Koning, B., Dionisi-Vici, C., and Williams, M.; additional individual contributors of MetabERN (2021). Liver and/or kidney transplantation in amino and organic acid-related inborn errors of metabolism: An overview on European data. J. Inherit. Metab. Dis. *44*, 593–605. https://doi.org/10.1002/jimd.12318.

36. Pillai, N.R., Stroup, B.M., Poliner, A., Rossetti, L., Rawls, B., Shayota, B.J., Soler-Alfonso, C., Tunuguntala, H.P., Goss, J., Craigen, W., et al. (2019). Liver transplantation in propionic and methylmalonic acidemia: A single center study with literature review. Mol. Genet. Metabol. *128*, 431–443. https://doi.org/10.1016/j.ymgme.2019.11.001.

37. Carrillo-Carrasco, N., Chandler, R.J., Chandrasekaran, S., and Venditti, C.P. (2010). Liver-directed recombinant adeno-associated viral gene delivery rescues a lethal mouse model of methylmalonic acidemia and provides long-term phenotypic correction. Hum. Gene Ther. *21*, 1147–1154. https://doi.org/10.1089/hum.2010.008.

38. Chandler, R.J., and Venditti, C.P. (2010). Long-term rescue of a lethal murine model of methylmalonic acidemia using adeno-associated viral gene therapy. Mol. Ther. *18*, 11–16. https://doi.org/10.1038/mt.2009.247.

39. Chandler, R.J., and Venditti, C.P. (2012). Pre-clinical efficacy and dosing of an AAV8 vector expressing human methylmalonyl-CoA mutase in a murine model of methylmalonic acidemia (MMA). Mol. Genet. Metabol. *107*, 617–619. https://doi.org/10.1016/j.ymgme.2012.09.019.

40. Guenzel, A.J., Hillestad, M.L., Matern, D., and Barry, M.A. (2014). Effects of adeno-associated virus serotype and tissue-specific expression on circulating biomarkers of propionic acidemia. Hum. Gene Ther. *25*, 837–843. https://doi.org/10.1089/hum.2014.012.

41. Subramanian, C., Frank, M.W., Tangallapally, R., Yun, M.K., White, S.W., Lee, R.E., Rock, C.O., and Jackowski, S. (2023). Relief of CoA sequestration and restoration of mitochondrial function in a mouse model of propionic acidemia. J. Inherit. Metab. Dis. *46*, 28–42. https://doi.org/10.1002/jimd.12570.

42. Cunningham, S.C., Spinoulas, A., Carpenter, K.H., Wilcken, B., Kuchel, P.W., and Alexander, I.E. (2009). AAV2/8-mediated correction of OTC deficiency is robust in adult but not neonatal Spf(ash) mice. Mol. Ther. *17*, 1340–1346. https://doi.org/10.1038/mt.2009.88.

43. Wang, L., Bell, P., Lin, J., Calcedo, R., Tarantal, A.F., and Wilson, J.M. (2011). AAV8-mediated hepatic gene transfer in infant rhesus monkeys (Macaca mulatta). Mol. Ther. *19*, 2012–2020. https://doi.org/10.1038/mt.2011.151.

44. Chen, P.J., and Liu, D.R. (2023). Prime editing for precise and highly versatile genome manipulation. Nat. Rev. Genet. *24*, 161–177. https://doi.org/10.1038/s41576-022-00541-1.

45. Marcell, P.D., Stabler, S.P., Podell, E.R., and Allen, R.H. (1985). Quantitation of methylmalonic acid and other dicarboxylic acids in normal serum and urine using capillary gas chromatography-mass spectrometry. Anal. Biochem. *150*, 58–66. https://doi.org/10.1016/0003-2697(85)90440-3.

46. Allen, R.H., Stabler, S.P., Savage, D.G., and Lindenbaum, J. (1993). Elevation of 2-methylcitric acid I and II levels in serum, urine, and cerebrospinal fluid of patients with cobalamin deficiency. Metabolism *42*, 978–988. https://doi.org/10.1016/0026-0495(93)90010-l.

OMTM, Volume *30*

Supplemental information

Systemic gene therapy using an AAV44.9 vector rescues a neonatal lethal mouse model of propionic acidemia

Randy J. Chandler, Giovanni Di Pasquale, Eun-Young Choi, David Chang, Stephanie N. Smith, Jennifer L. Sloan, Victoria Hoffmann, Lina Li, John A. Chiorini, and Charles P. Venditti

Table S1. Relative hepatic and cardiac PCCA protein levels

Genotype	Liver	Heart
Pcca$^{+/+}$ (n=2)	100±2.4	100±20.3
Pcca$^{-/-}$ (n=2)	ND	ND
Pcca$^{-/-}$ + AAV44.9 (n=3)	44.7±4.4	214.3±18.9

PCCA protein levels from Figure 4D shown as a mean percentage±SEM of *Pcca*$^{+/+}$ wildtype PCCA protein levels after normalization with ACTB (liver) or GAPDH (heart).

A.

NM_144844.2 Mus musculus *Pcca* var1 with c.398_401delAAGC mutation

ATGGCGGGGCAGTGGGTCAGGACCGTGGCGCTGTTGGCGGCCAGGCGGCATTGGCGGCGGT
CCTCGCAGCAGCAATTGCTGGGGACGCTGAAGCATGCTCCAGTCTATTCATACCAATGCCTA
GTGGTGTCCAGAAGTCTCAGTTCTGTGGAATATGAGCCTAAAGAAAAGACTTTTGATAAAAT
TCTCATTGCTAACAGAGGAGAAATTGCCTGTAGGGTTATTAAAACTTGCAAGAAGATGGGCA
TCAAGACAGTTGCCATTCACAGTGATGTTGATGCCAGTTCTGTTCACGTGAAAATGGCGGAT
GAGGCTGTCTGTGTTGGCCCAGCTCCCACCAGTAAAAGCTACCTCAACATGGATGCCATCAT
GGAAGCCATTAAGAAAACCAGGGCCCTGTACACCCAGGGTATGGATTCCTGTCAGAAAACA
AAGAGTTTGCAAAGCGTCTGGCAGCAGAAGATGTCACTTTCATTGGACCTGATACTCATGCT
ATTCAAGCCATGGGTGACAAGATAGAAAGCAAACTATTAGCCAAGAGAGCAAAGGTCAACA
CAATCCCTGGTTTTGATGGGGTAGTAAAGGATGCAGATGAAGCTGTCAGAATTGCAAGGGA
AATTGGCTACCCTGTGATGATCAAGGCCTCAGCAGGCGGTGGTGGGAAAGGCATGCGCATC
GCCTGGGATGACGAAGAGACCAGGGATGGCTTTAGATTTTCATCCCAGGAAGCTGCTTCTAG
TTTTGGTGATGATAGACTACTAATAGAAAAATTTATCGATAACCCTCGTCATATAGAAATCC
AGGTTTTAGGGGATAAACATGGCAATGCTCTGTGGCTCAATGAGAGGGAGTGCTCGATCCA
GAGAAGGAACCAGAAGGTGGTAGAGGAGGCGCCAAGCATTTTTCTGGATCCTGAAACTCGC
CAAGCAATGGGAGAGCAGGCCGTGGCTTTGGCTAAAGCCGTGAAGTATTCTTCTGCTGGAAC
TGTGGAATTTCTTGTGGACTCCCAGAAGAATTTTTACTTCTTGGAGATGAATACAAGACTAC
AGGTCGAACATCCTGTCACAGAGTGCATTACTGGCCTGGACTTAGTCCAAGAAATGATCCTT
GTTGCTAAGGGTTACCCACTCAGGCACAAGCAAGAGGATATTCCCATCAGTGGCTGGGCAGT
TGAATGTCGGGTTTATGCTGAGGACCCCTACAAGTCTTTCGGTTTACCGTCTATTGGGAGGCT
GTCCCAGTACCAAGAGCCGATACATCTACCTGGTGTCCGAGTTGACAGTGGCATCCAACCAG
GAAGTGACATCAGCATCTATTATGATCCTATGATTTCAAAGCTAGTCACATATGGGTCTGAC
AGAGCAGAAGCCCTGAAGAGGATGGAAGACGCACTGGACAATTATGTGATCCGGGGTGTTA
CACACAACATCCCATTGCTCCGGGAGGTGATAATCAACACACGTTTTGTGAAAGGAGACATC
AGCACTAAGTTTCTCTCTGATGTGTATCCTGATGGCTTCAAAGGGCACACGTTAACACTGAG
TGAGAGAAACCAGTTATTGGCCATTGCATCATCTGTATTTGTGGCATCCCAGCTACGAGCTC
AGCGCTTCCAAGAACATTCAAGAGTACCAGTTATTAGGCCTGATGTGGCTAAGTGGGAGCTC
TCGGTAAAGTTACATGATGAAGATCATACTGTCGTGGCATCTAACAATGGGCCGGCATTTAC
CGTGGAAGTTGATGGCTCGAAACTAAATGTGACCAGTACGTGGAACCTGGCGTCACCCTTAT
TGTCTGTCAACGTTGATGGCACGCAGAGGACTGTGCAGTGTCTTTCTCGGGAAGCAGGTGGA
AACATGAGCATCCAGTTTCTTGGCACAGTGTACAAAGTGCACATTTTAACCAAGCTTGCTGC
AGAGCTGAACAAATTCATGCTTGAAAAAGTGCCCAAGGACACCAGCAGCACTCTGTGCTCC
CCGATGCCTGGAGTGGTGGTGGCCGTTTCTGTCAAGCCTGGAGACATGGTAGCAGAAGGTCA
GGAAATCTGTGTGATTGAAGCTATGAAAATGCAGAACAGTATGACAGCTGGGAAAATGGGC
AAGGTGAAATTGGTGCACTGCAAAGCTGGAGACACAGTTGGTGAAGGAGACCTGCTTGTGG
AGCTGGAATGA

B.

Predicted PCCA protein p.Gln133Leufs*41

MAGQWVRTVALLAARRHWRRSSQQQLLGTLKHAPVYSYQCLVVSRSLSSVEYEPKEKTFDKILI
ANRGEIACRVIKTCKKMGIKTVAIHSDVDASSVHVKMADEAVCVGPAPTSKSYLNMDAIMEAIK
KTRALYTQGMDSCQKTKSLQSVWQQKMSLSLDLILMLFKPWVTR*

Figure S1. DNA and Protein Sequence of new murine *Pcca* PA disease allele A. cDNA sequence of NM_144844.2 Mus musculus *Pcca* var1 with c.398_401delAAGC mutation **B.** Predicted amino acid of sequence of PCCA p.Gln133Leufs*41

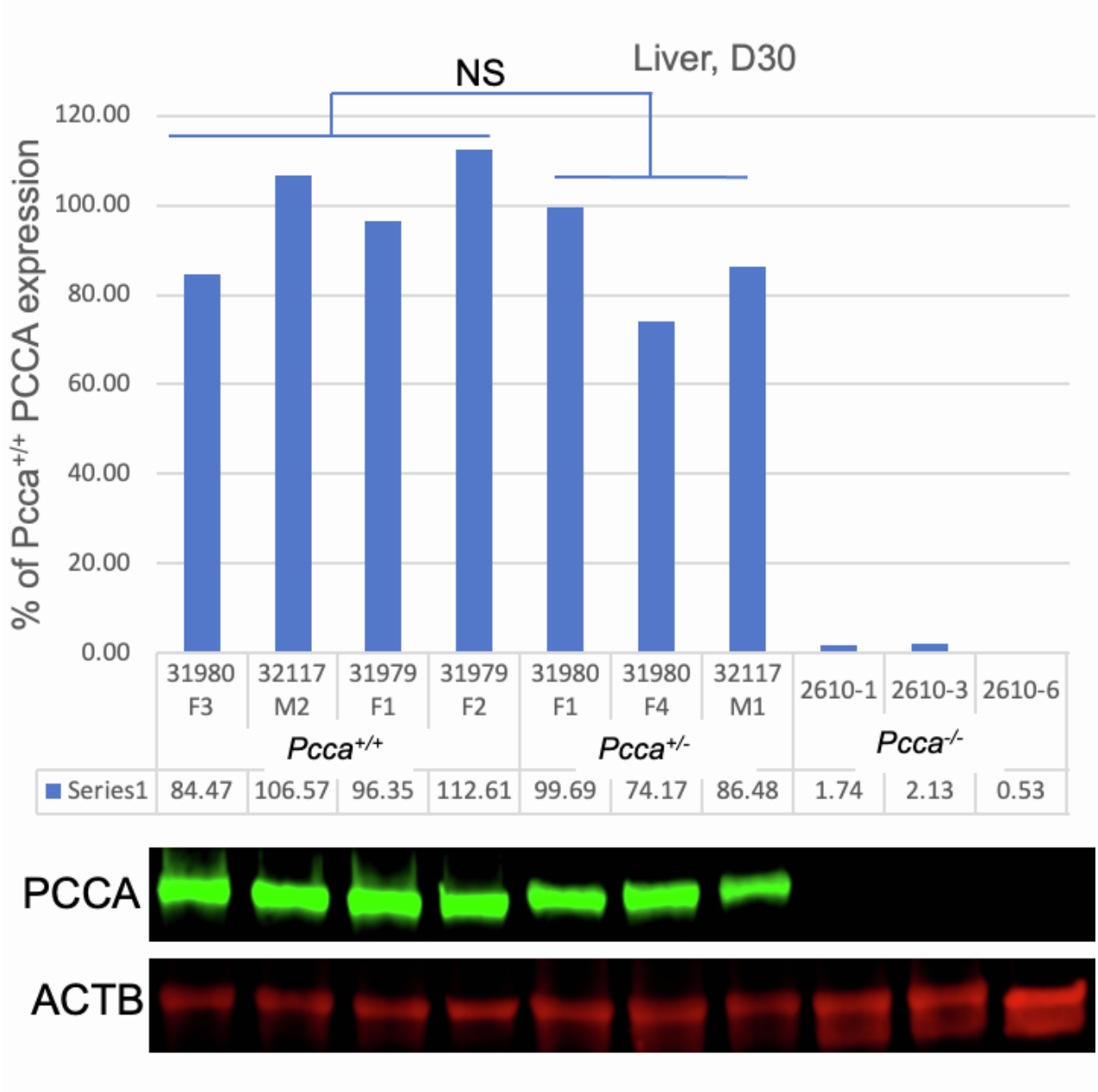

Figure S2. Immunoblot of 50 µg hepatic protein from a *Pcca*$^{+/+}$, *Pcca*$^{+/-}$ and a *Pcca*$^{-/-}$ newborn pups for the PCCA protein using ACTB as a loading control. The amount of PCCA protein expression from the immunoblot was used to determine the percent of the wildtype PCCA expression after normalization with the loading control using ImageJ software

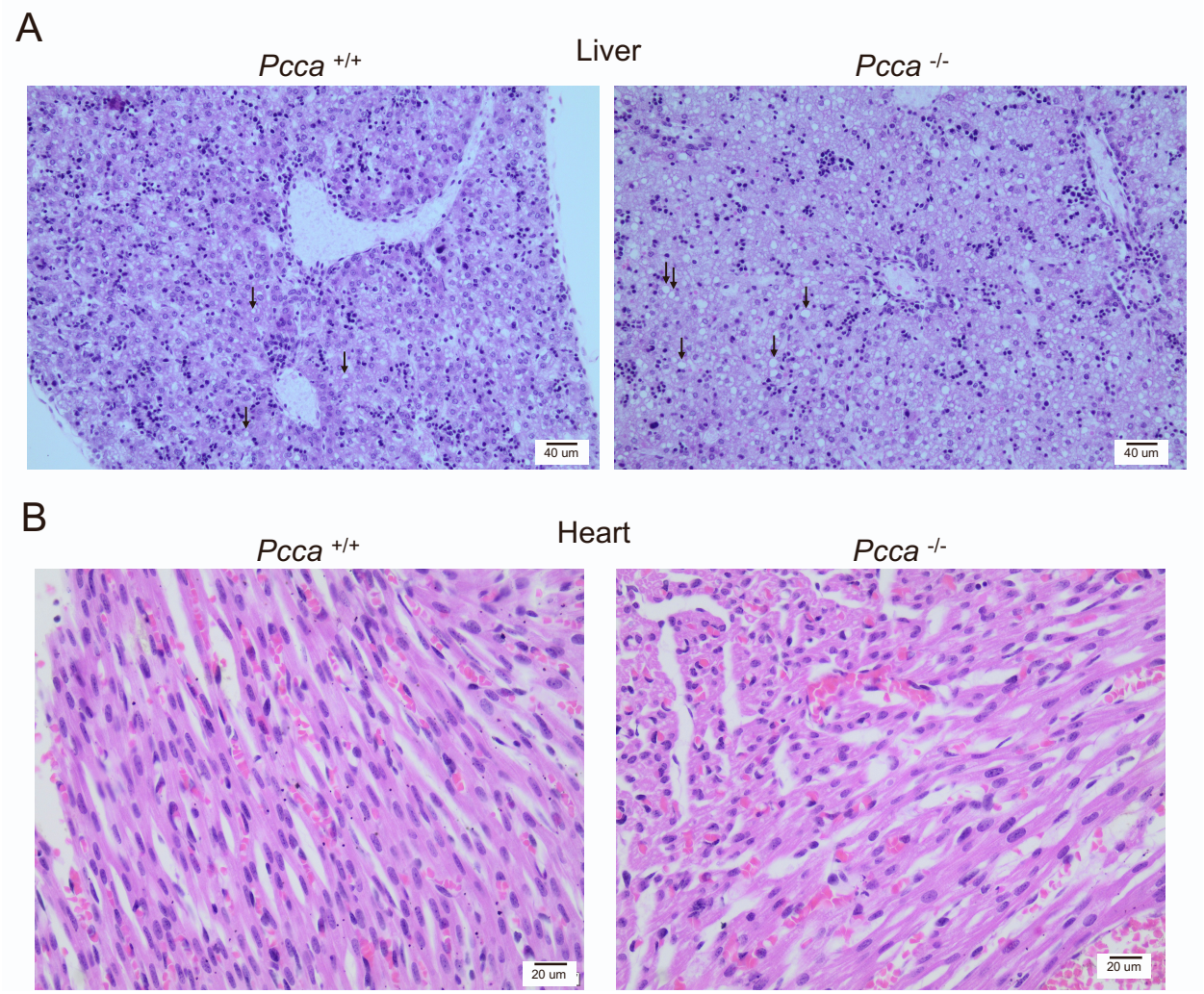

Figure S3. Liver and heart histopathology. A. Liver (10X) H&E stained neonatal *Pcca*$^{-/-}$ mice (untreated day of life 1) have diffuse mixed microvesicular and macrovesicular lipidosis (see as clear vacuoles indicated by arrows) compared to *Pcca* $^{+/+}$ mice. **B.** Heart (20X) H&E stained tissues from *Pcca*$^{-/-}$ and *Pcca* $^{+/+}$ mice (untreated day of life 1). No notable changes in the *Pcca*$^{-/-}$ mice were noted.

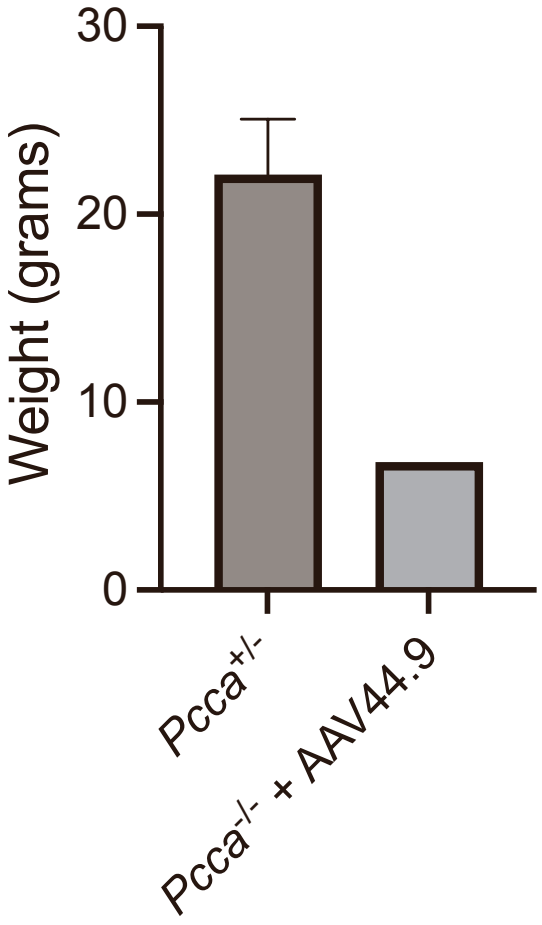

Figure S4. Weight of AAV44.9 treated litter mates. *Pcca*$^{+/-}$ (n=2) and a *Pcca*$^{-/-}$ (n=1) AAV44.9 treated male littermates at 2 months of age.

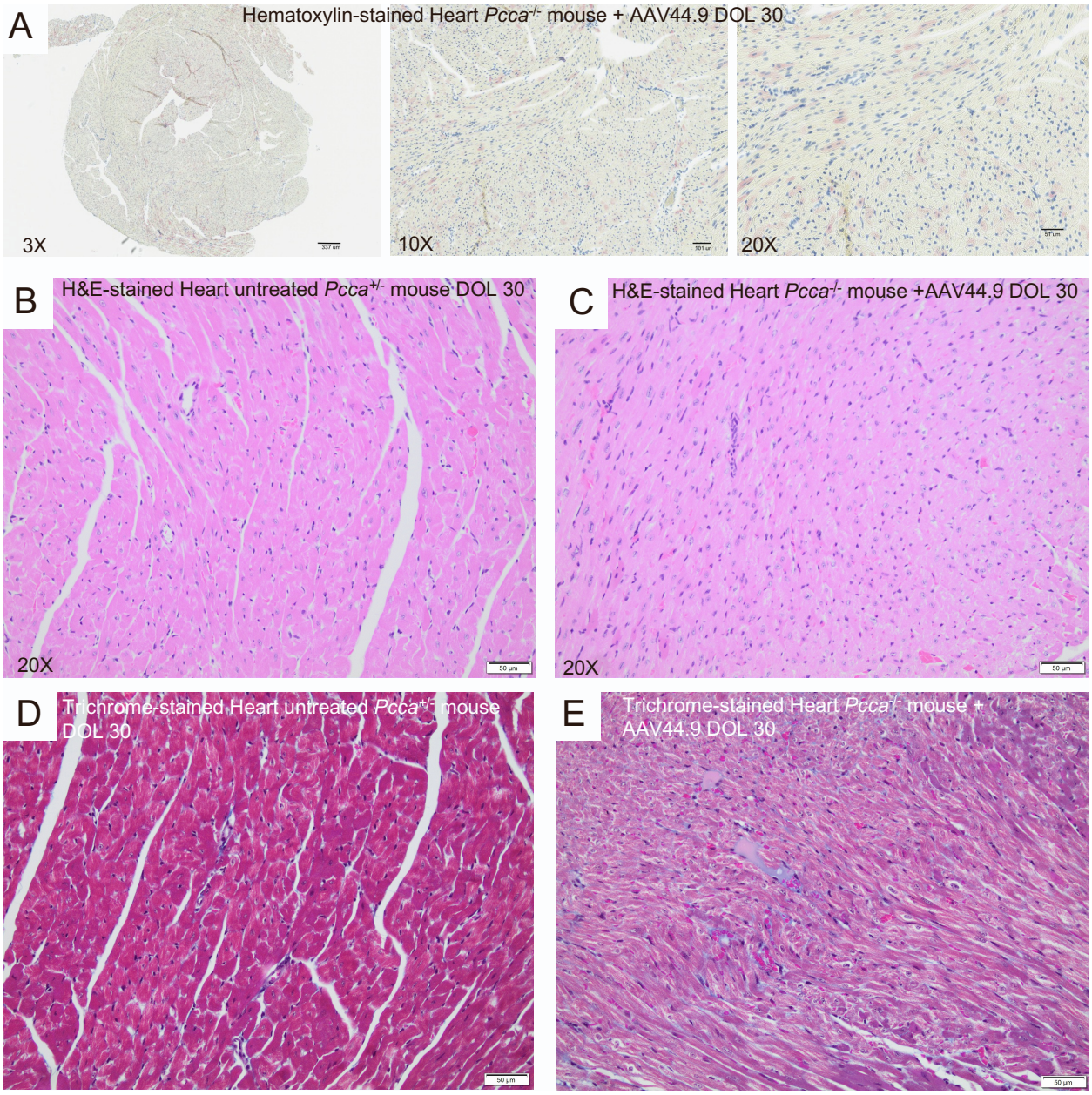

Figure S5. Cardiac histology. A. Hematoxylin-stained heart from a AAV44.9 treated *Pcca*$^{-/-}$ mice DOL 30 Heart 3X, 10X and 20X (left to right). **B.** H&E-stained heart DOL 30 wildtype (*Pcca*$^{+/-}$) untreated control 20X. **C.** H&E-stained heart DOL 30 *Pcca*$^{-/-}$ AAV44.9 treated mouse. **D.** Trichrome DOL 30 wildtype (*Pcca*$^{+/-}$) untreated control. **E.** Masson's Trichrome stained heart DOL 30 *Pcca*$^{-/-}$ AAV44.9 treated mouse. No notable changes in the *Pcca*$^{-/-}$ mice were noted in any of the stains. *Pcca*$^{-/-}$ mouse was treated with a dose of 1e11vg at DOL1. DOL (Day of life)